

Article

Experimental Evaluation of the Bending Behavior of a Drilled Shaft with Partial Casing under Lateral Loads

Xiaojuan Li ¹ , Guoliang Dai ^{2,3,*}, Xueying Yang ^{2,3}, Qian Yin ^{2,3}, Wenbo Zhu ^{2,3} and Fan Zhang ^{2,3}

¹ School of Civil Engineering and Architecture, Jiangsu University of Science and Technology, Zhenjiang 212003, China; Xiaojuan_li05@outlook.com

² Key Laboratory for RC and PRC Structure of Education Ministry, Nanjing 210096, China; 230208612@seu.edu.cn (X.Y.); 230198808@seu.edu.cn (Q.Y.); 230169390@seu.edu.cn (W.Z.); 230198122@seu.edu.cn (F.Z.)

³ School of Civil Engineering, Southeast University, Nanjing 210096, China

* Correspondence: daigl@seu.edu.cn

Abstract: Few studies, especially those related to field tests, have examined the bending behaviors of drilled shafts with partial casings (DSPCs). This work reports the results of experimental studies on the behavior of DSPCs under lateral loads, including an in situ test and a set of laboratory tests. First, a DSPC with a diameter of 2 m and length of 87.9 m was studied in clay beds, and a steel casing with a diameter of 2.0 m and length of 33 m was used. In this test, strain gauges were distributed along the steel rebars in the concrete pile and the wall of the steel tube at different depths, and thus the longitudinal strains of the concrete pile and the steel tube could be studied. Second, laboratory experiments were implemented with reinforced concrete-filled steel tubular columns under pure bending conditions. In these tests, strain gauges were distributed along the steel rebars in the concrete pile and the walls of the steel tubes at the pure bending section of the specimens. Different wall thicknesses and drilling fluid conditions were considered. The field test results show that the strain of the concrete piles and the steel tubes were linearly distributed at the same cross-section. This means that a DSPC remains a flat plane after it deforms. Whereas a correction coefficient related to the loading level need to be considered in the calculation of the bending stiffness. Laboratory studies show that the strain of DSPCs was linearly distributed at a small bending moment under the best bond-quality condition, whereas obvious nonlinear behaviors were shown under a large bending moment with poor bond-quality conditions.

Keywords: reinforced concrete pile; partial casing; in situ test; laboratory test; bending behavior



Citation: Li, X.; Dai, G.; Yang, X.; Yin, Q.; Zhu, W.; Zhang, F. Experimental Evaluation of the Bending Behavior of a Drilled Shaft with Partial Casing under Lateral Loads. *Appl. Sci.* **2021**, *11*, 9469. <https://doi.org/10.3390/app11209469>

Academic Editor: Daniel Dias

Received: 10 September 2021

Accepted: 7 October 2021

Published: 12 October 2021

Publisher's Note: MDPI stays neutral with regard to jurisdictional claims in published maps and institutional affiliations.



Copyright: © 2021 by the authors. Licensee MDPI, Basel, Switzerland. This article is an open access article distributed under the terms and conditions of the Creative Commons Attribution (CC BY) license (<https://creativecommons.org/licenses/by/4.0/>).

1. Introduction

Cast in situ concrete piles (CCPs) have been widely used in bridge projects to bear complex and large loads, especially the lateral load and overturning moment. During the cast in situ concrete pile construction process, steel casings are widely used. However, in some projects, these tubes cannot be removed before grouting. This will form a drilled shaft with partial casing (DSPC). Fortunately, it was found that these piles are more supportable than traditional CCPs. For example, in the Tai Zhou Bay Super Bridge of China, the lateral force from the upper bridge was so large that it caused a large bending moment in the pile foundation, of which the section strength could not bear; a similar phenomenon has been observed in the Hong Kong–Zhuhai–Macao Bridge. Some research has also been conducted on similar improvements for concrete-filled steel columns [1] and concrete plugs embedded in tubular steel piles [2,3].

DSPCs have some differences from traditional CCPs, concrete-filled steel columns, or concrete plugs embedded in tubular steel piles [2,4,5]. In a DSPC, the steel casing is partially used (Figure 1); then, a hole is drilled in the casing, and the soil in the tube is removed by the slurry method. This may result in a weak bond between the concrete

body and steel tube in the composite structure. Many results have been reported about the bond stress capacity of concrete-filled steel columns. In these studies, the different shapes of column sections were tested [6,7], and the interface length, interface condition [8], mechanical connectors, and diameter-to-thickness (D/t) ratio were also studied [9–12]. However, few of them have investigated the assumed plane cross-section effect on the bending capacity of DSPCs, the mud effect on the bond strength, and the mechanical interlocking of concrete–steel interfaces under bending conditions.

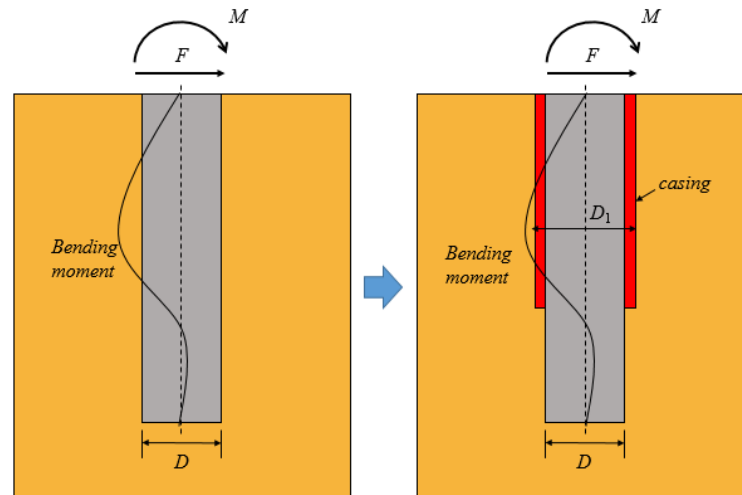


Figure 1. Monopile with casing and without casing.

Therefore, in this study, a set of experimental programs regarding the Tai Zhou Bay Super Bridge was introduced. A DSPC with a diameter of 2 m, length of 87.9 m, a steel tube diameter of 2.0 m, and a length of 33 m was studied in clay beds. Strain gauges were distributed along the steel rebars in the concrete pile and at the surface of the steel tube at the same cross-sections along different embedment depths. Therefore, the longitudinal strains of the concrete pile and steel tube can be studied separately. Moreover, a set of laboratory experiments were implemented. They are reinforced concrete-filled steel tubular columns (RCFSTCs) under pure bending conditions. In these tests, strain gauges were distributed along the steel rebars in the concrete pile and at the wall of the steel tube at the pure bending section of these RCFSTCs. Different wall thicknesses and mud conditions were considered to study the influence of the bonding quality on the bending capacity.

2. Experimental Program for Field Tests

2.1. Experimental Procedure

A cast in situ reinforced concrete pile with a partial steel casing was load tested at a bridge construction site located in the coastal area of Zhejiang, China. The cast in situ pile had a designed diameter of 1.8 m and an embedment length of 87.9 m. In the pile body, reinforcement bars with a nominal yield strength of 300 MPa and an ultimate tensile strength of 350 MPa were used. The casing had an outer diameter of 2 m, a thickness of 0.075 m, and an embedment depth of 33 m (Figure 2). The casing had a nominal yield strength of 300 MPa and an ultimate tensile strength of 350 MPa. Therefore, the test pile had an outer diameter of 2.0 m at depths from 0 m to -33.0 m and an inner diameter of 1.8 m from -33.0 m to -87.9 m.



Figure 2. Angle steel outside the steel casing.

Sliding microtiters (Solexperts AG, Mönchaltorf, Switzerland), vibrating wire strain gauges, and inclinometers (CX901F, China) were used to measure the axial strain of the casing and the concrete (Figure 2). Seven steel-angled channels with a length of 22 m were welded onto the outer surface of the casing, five of which were used for inclinometers, and another two were used for sliding microtiters. The bottoms of these channels were covered by tapered steel bases to prevent soil intrusion during the casing driving process (the driving was accomplished with a hammer). Grouting was performed in channels to keep these instruments and the casing in cooperative deformation conditions. The rebar cage was also installed with inclinometer tubes and strain gauges to measure the deflection of the concrete. Strain gauges were attached evenly around the pile at 9 different depths along the pile length. For each depth, 4 gauges were attached evenly around the cross-section. The layout of the strain gauges is shown in Figure 3.

Adjacent to the test pile, there was another pile, and the loads were applied through a jack placed between the two piles as a counter force system. A jack with a 60 MPa capacity and precision of 0.4 MPa was used to provide lateral load to the test pile. This gave a comfortable margin of capacity over the designed ultimate lateral force of the pile of 1000 kN. Four dial gauges were used on the opposite side of the loading point to survey the lateral deflection of the pile top under different loading conditions (Figure 3).

The construction of the pile generally contains the following four procedures: (1) drive a casing, (2) drill a hole, (3) deploy a rebar cage, and (4) fill the hole with concrete.

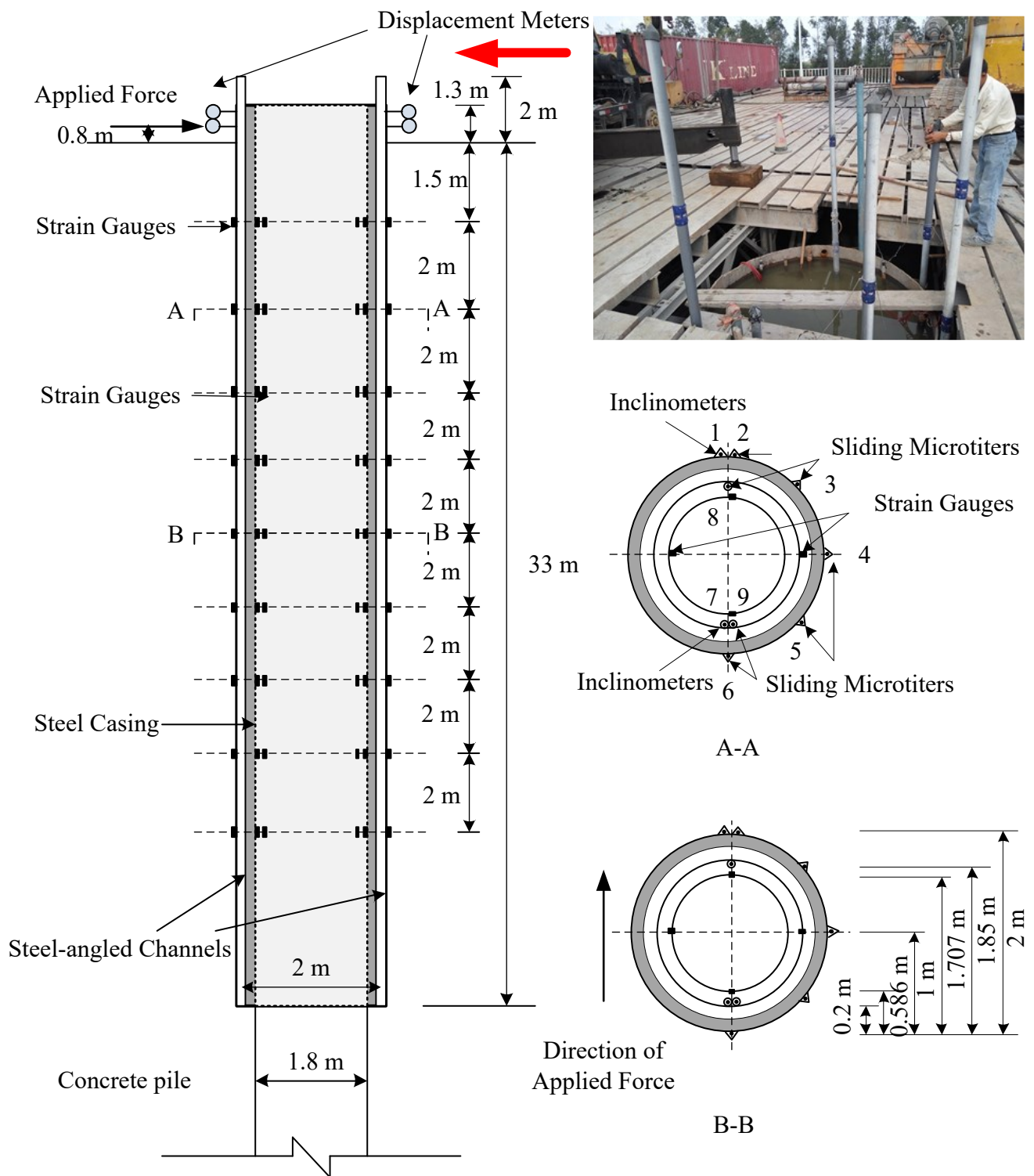


Figure 3. The layout of the instrumentations.

2.2. Test Results

The purpose of the field test is to evaluate the pile section with the maximum bending moment and to verify the plane cross-section assumption. From the deflection profiles in Figure 4a, we can see that the data from inclinometers and those from sliding micrometers agreed with each other, which means that the casing and the concrete body of the pile bent as an assembly. The bending moment along the pile and the casing is shown in Figure 4b.

From the bending moment profile curves, we can be assured that the maximum bending moment existed in the casing-covered pile section at depths from 11 to 14 m. The larger the applied force was, the deeper the maximum bending moment appeared. It should be noted that the value may not be the real bending moment, and we merely care about the position where the maximum bending moment appeared. Therefore, as seen from Figure 2, the depth of 12 m where the strain gauges were attached was the nearest measurement section in the pile body. The distribution of strain along the cross section is given in Figure 5.

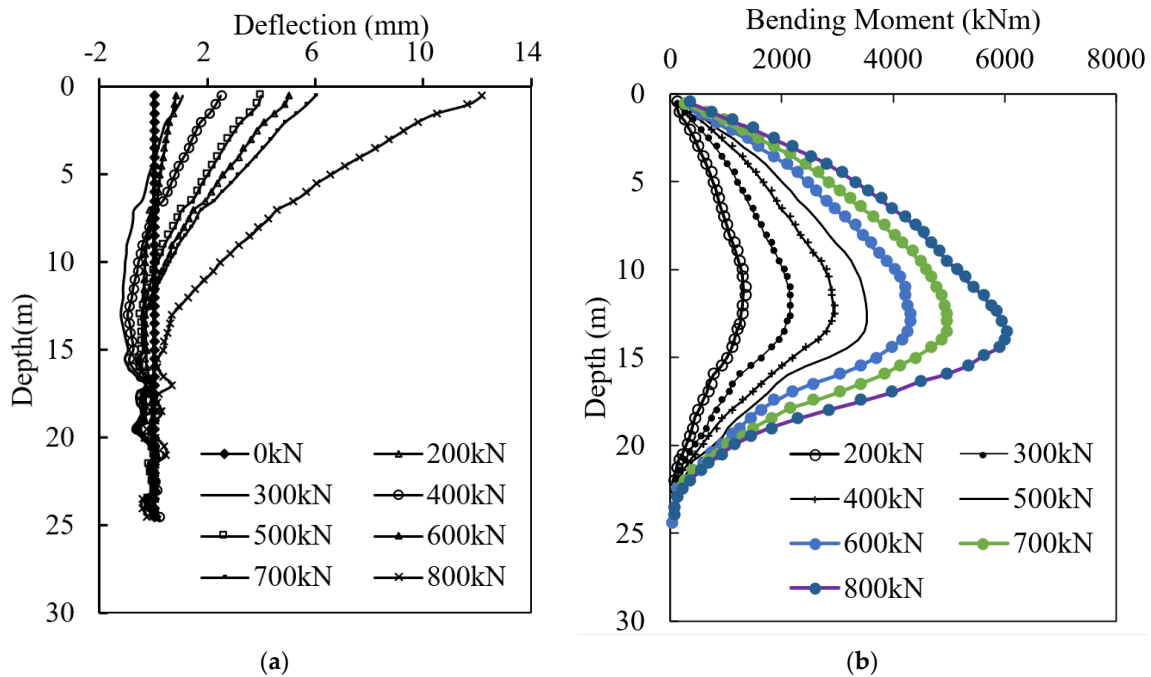


Figure 4. (a) Deflection vs. depth and (b) bending moment vs. depth.

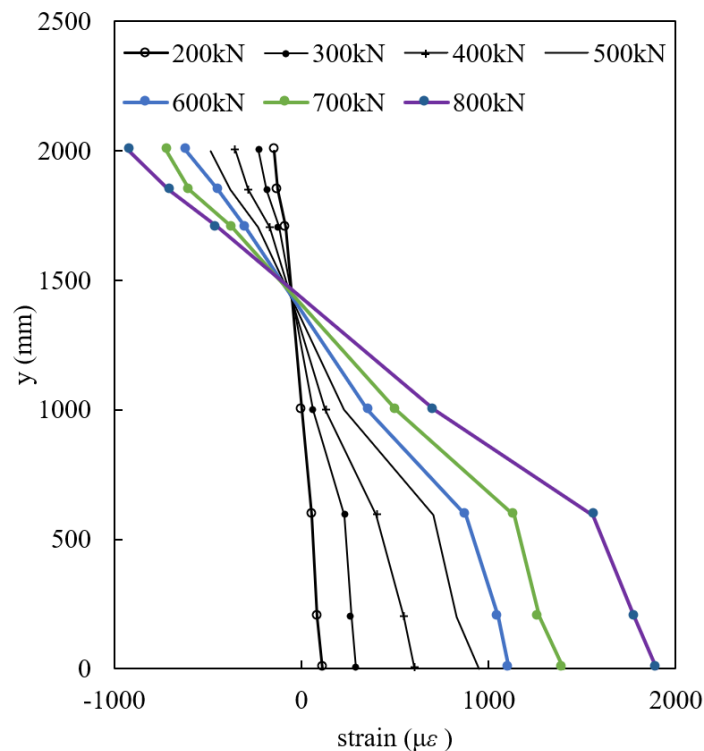


Figure 5. The distribution of strain along pile cross-section.

In Figure 5, the x-label is the distribution of strain along the cross section of the DSPC at the depth of 12 m; the values were from sliding microtiters, vibrating-wire strain gauges, and inclinometers found in Figure 4. The y-label is the height of the pile section. All the points are linearly distributed at different loading stages; the closer the measurement points were to the surface of the pile body, the larger the strain was. It is obvious that there was no relative displacement between the concrete and the casing during the loading process. This means that the casing and the concrete body deformed as an assembly. It is reasonable to use the plane cross-section assumption in the calculation of the bending stiffness.

For the rigid stiffness of steel-concrete piles, the calculation method is as follows:

$$EI = E_s I_s + \eta E_p I_p \quad (1)$$

where E_s is the modulus of elasticity of the steel casing, I_s is the moment of inertia of the steel casing, $E_p I_p$ is the bending stiffness of the concrete pile, and η is the correction coefficient. There are different η values for different criteria, such as Chinese codes [13], with a value of 1.0. In Japan [14], this value is 0.2, and in Europe [15], it is 0.6.

The initial bending stiffness $E_p I_p$ of the DSPC is calculated as follows:

$$EI = E_s I_s + E_p I_p = 5.92 \times 10^{10} \text{ N}\cdot\text{m}^2 \quad (2)$$

where $E_s I_s = E_s \pi (d_1^4 - d^4) / 64$; $E_p I_p = 0.85 E_c \pi d (d^2 + 2(a_E - 1) \rho_g d_0^2) / 32$; d_1 is the diameter of the outside casing, $d_1 = 2.0$ m; d is the pile diameter, $d = 1.8$ m; d_0 is the net diameter that does not include the thickness of the cover, $d_0 = 1.64$ m; a_E is the ratio of the modulus of elasticity of the steel bar to that of the concrete, $a_E = E_s / E_c = 5.56$; ρ_g is the reinforcement ratio of the pile body, $\rho_g = 0.57\%$, $E_s = 2.1 \times 10^5$ MPa; and E_c is the modulus of elasticity of the concrete, $E_c = 3.6 \times 10^4$ MPa.

Figure 6 shows the bending moment-stiffness response of pile section 0.3 below the loading point. The x-label is the ratio of the bending moment at the pile section and the maximum value, M/M_{\max} , where $M = Fh$, F is the lateral force, h is 0.3 m, and M_{\max} is 240 kNm. The y-label is the ratio of bending stiffness (α) at the pile section and the maximum value, where $\alpha = (EI)_{\text{measured}} / EI$, $(EI)_{\text{measured}} = M / (dw^2/d^2z)$, w is the deflection of pile (Figure 4), and z is the depth (m).

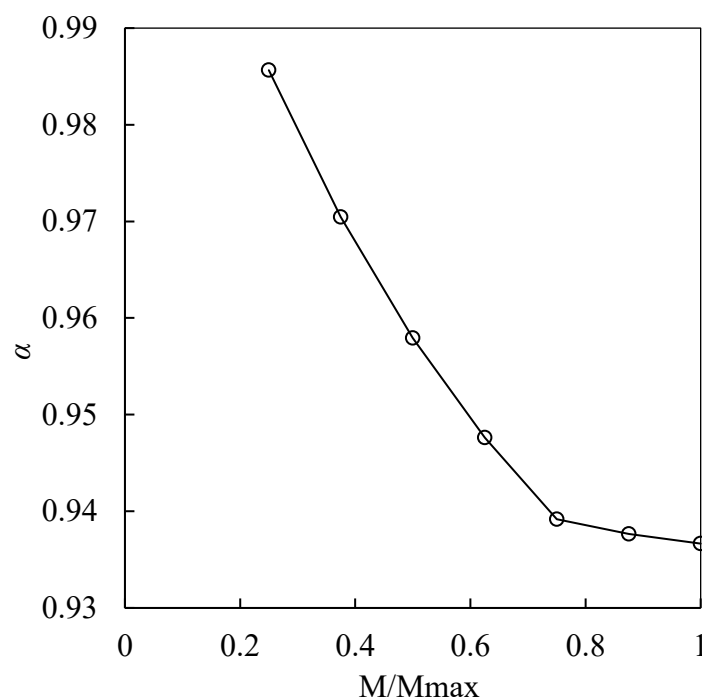


Figure 6. The bending moment-stiffness response of pile section 0.3 below loading point.

From the above figure, we find that the bending stiffness of the pile section changed with the loading level. The bending stiffness decreased with the lateral loading level and remained stable at $M/M_{\max} = 1$, where $\alpha = 0.937$. This means that it is more reasonable to consider a correction coefficient, which is related to the loading level, in the calculation of the bending stiffness.

However, the test pile would become a part of the bridge, and it is impossible to study the pile during a field test until the collapse of the structure or the loss of serviceability, and therefore the interaction between the pile and the casing under such high loads cannot be tested. Moreover, the influences of the casing thickness and slurry quality during pile construction on the moment capacity of DSPCs are unknown. To completely investigate the impact of the slip between the concrete and casing of piles on the bending capacity of DSPCs, we implemented bending tests of pile specimens in the following study.

3. Laboratory Tests

According to a standard procedure of making a DSPC, the slurry would weaken the bonding quality between the casing and the concrete pile if the hole was not cleaned thoroughly before filling concrete. However, from the field test, because of the limited level of lateral loading levels, the casing and the concrete worked together as a whole part. To further study the influence of bonding quality and the thickness of the casing on the bending behavior of DSPCs, we conducted six specimen tests under pure bending conditions. The purpose was to determine these effects on the bending capacity of the specimens and to determine whether the plane cross-section assumption is suitable for larger loads.

3.1. Experimental Procedure

A total of six specimens were prepared and tested to study the influence of bonding properties on the bending performance. The geometry and materials were identical. Steel tubes with a nominal yield strength of 235 MPa, ultimate tensile strength of 412 MPa, elastic modulus of 210 GPa, and Poisson's ratio of 0.286 were used, and the related parameters are shown in Table 1. These steel tubes have an outer diameter of 426 mm, wall thickness of 5 mm or 10 mm, and total length of 4 m. The inner surfaces of the steel tubes were cleaned and filled with concrete. The results from the concrete property test revealed a compressive strength of 62.6 MPa at an age of 28 days.

Table 1. Relative parameters of the steel casing.

Material Type	Modulus of Elasticity E/GPa	Poisson's Ratio ν	Yield Strength f_y/MPa	Tensile Strength f_u/MPa
Q235b	210	0.286	235	412

Similarly, the reinforcing cages used in these specimens were the same. Each of them consisted of four longitudinal bars (16 mm diameter with nominal yield strength of 400 MPa) and hooping (10 mm diameter with nominal yield strength of 300 MPa). As shown in Figure 7a, the side length of hooping was 255 mm. Hooping was installed at four sections of each specimen, which were 0.2 m, 1.2 m, 2.8 m, and 3.8 m in length. Because of the construction conditions, the shape of the hoop was rectangular, which was not like the test pile used in the field test. While we focused on the interface effect of concrete and steel casing on the bending capacity of specimens, the effect of hooping shape had a limited effect on this.

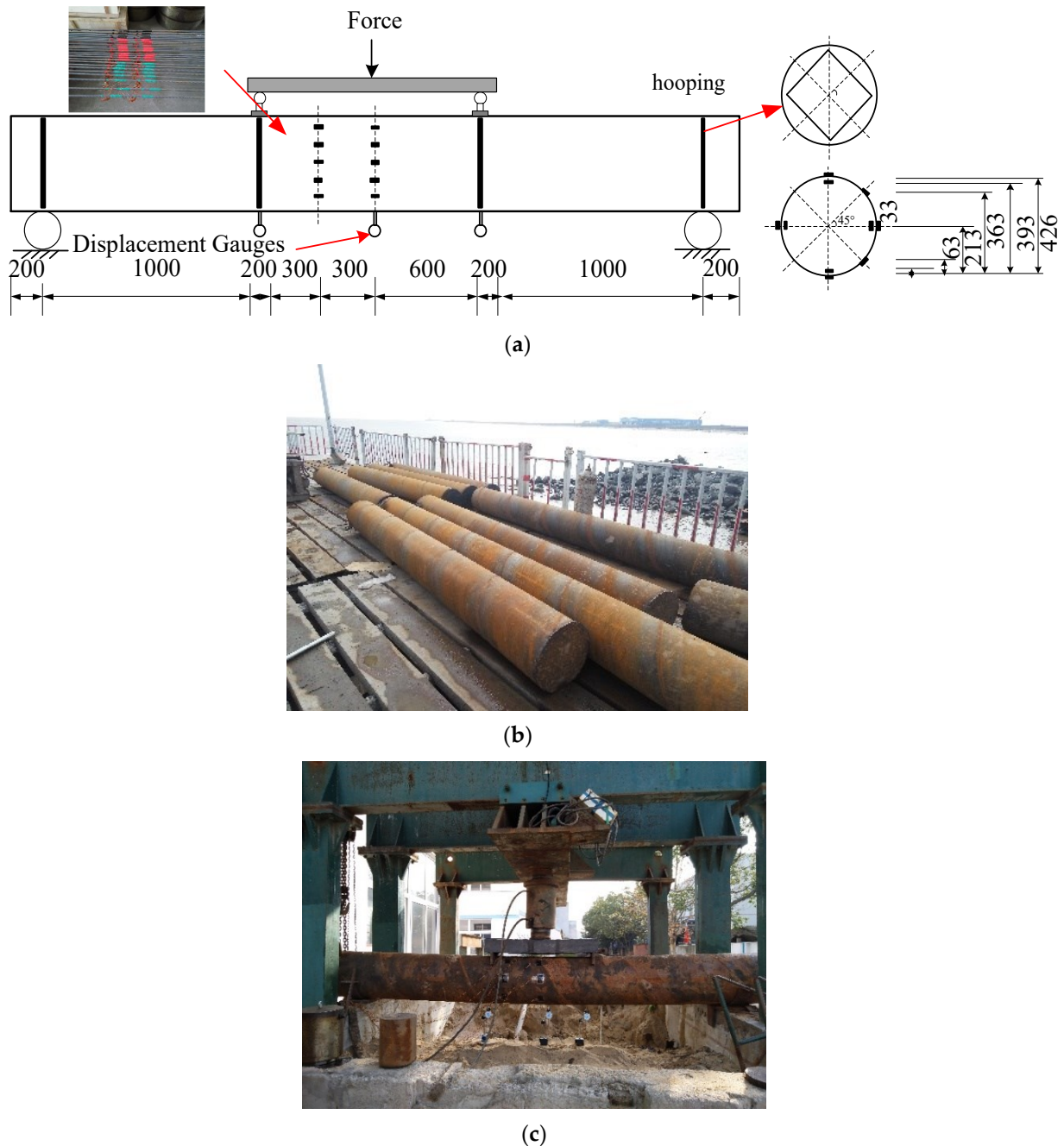


Figure 7. The layout of (a) strain gauges, (b) specifications and (c) dial gauges.

The specifications of the constructed specimens are summarized in Table 2. Groups B1, B3, and B5 were prepared to evaluate the effect of slurry conditions on the moment capacity of piles; groups B2, B4, and B6 were prepared for the same purpose. Groups B1 and B2 were prepared to evaluate the effect of casing thickness on the moment capacity of piles; groups B3, B4, B5, and B6 were prepared for the same purpose. The test setups of specimens B1 to B6 are shown in Figure 7c.

In order for a similar construction condition of the field test mentioned before to be simulated, those specimens should be merged into mud with different properties to form different bond qualities between the casings and the concrete. For the no-slurry skin condition, water was used instead; for the thin-slurry skin condition, the mud from the field test after the second hole cleaning was used, and the density was 1.15 g/cm^3 ; for the

thick-slurry condition, the mud after the first hole cleaning was used, and the density was 1.20 g/cm^3 .

Table 2. Test parameters of the specimens.

Specimen ID	Diameter (D/mm)	Thickness (t/mm)	Length (L/mm)	D/t	Mud Skin Condition
B-1	426	5	4000	85.2	no
B-2	426	10	4000	42.6	no
B-3	426	5	4000	85.2	thin
B-4	426	10	4000	42.6	thin
B-5	426	5	4000	85.2	thick
B-6	426	10	4000	42.6	thick

Strain gauges (BX120-4BB, China) and strain acquisition instruments (DH3816, China) were used to measure the strain of the concrete core and steel casing. The strain gauges were attached evenly around the reinforcement cage and the casing, which is shown in Figure 7a.

A vertical load was applied through a jack (shown in Figure 7c), which introduced a pure bending moment situation at the middle of the beam. Identical loads were applied at two points on the beam. As shown in Figure 7a, a concrete pool with a size of $4 \text{ m} \times 5 \text{ m} \times 4 \text{ m}$ was used as the loading table, and the specimens were 4 m long and hinged on it, which can restrict displacements of the ends. The distance between the two hinges was 3.6 m. Three dial gauges were installed at the opposite side of the loading point and at the middle of the span. The accumulation of the initial load was 10% of the ultimate load of specimens for each loading step and was kept for 2 min. When it was close to the failure state, the specimens were loaded slowly until failure.

As shown in Figure 7a, the measured sections were in the pure bending zone to monitor the strain of the casing and concrete. Ten strain gauges were used at the two sections to record the strains around the steel casing and in the concrete.

3.2. Test Results

The bending behavior of six specimens are similar. From Figure 8, failure always occurred at the loading points. There was no crack at the surface of the steel casing, but bending deformation could be observed in all specimens, which means that the steel casing was in the plastic stage at the end of loading. Removing the casing off the specimens, we observed micro vertical cracks in the concrete developing from the bottom to the top. The main shear cracks in the concrete core were observed around the loading points and the pure bending area, and the cracks at the bottom and top of the pile section are shown in Figure 8a. A simplified model is shown in Figure 8b, which describes how the casing and the concrete act in cooperation to resist the applied moment. It should be noted that no significant slippage occurred between the casing and the concrete, which almost kept in contact with each other throughout the entire loading period.

3.3. Effects of Different Parameters on the Bending Behaviour

3.3.1. Effect of the Bond Quality

During DSPC installation, slurry must be used to support the walls of the excavation. While the existence of mud would weaken the bond quality between the concrete and the casing, this may have a negative effect on the bending behavior of DSPCs. Therefore, it is necessary to study this factor.

From the results mentioned above, flexural failure was observed from those tests. Figure 9a shows comparisons of the bending moment-deflection curves of the beams with different mud conditions for two types of casing thicknesses. The bending moment at the central of the beam, M , is from the theory of a simply supported beam under concentrated loads. Groups B1, B3, and B5 were designed with the same materials and geometry (the

casing thickness was 5 mm), and the difference was the mud condition. B1 had no mud between the concrete and casing during construction, whereas B2 had worse bond quality and B3 had worse bond quality than B2. Groups B2, B4, and B6 were also designed with the same method (the casing thickness was 10 mm), and the difference was also the slurry condition.

As seen in Figure 9, the trends of the $M-\delta$ curves under different mud conditions were similar, which indicates that the bending behaviors of those specimens with different mud conditions were similar. However, it is interesting to see that the bending capacity shown in those curves was slightly influenced by the mud condition, the specimens with dilute mud condition showed the highest bending capacity, and those with no mud and thicker condition had lower but similar capacity. This implied that the mud condition had limited influence on the moment capacity of the specimens. The bonding strength between the casing and concrete was not an important factor with regard to the moment capacity of the specimens.

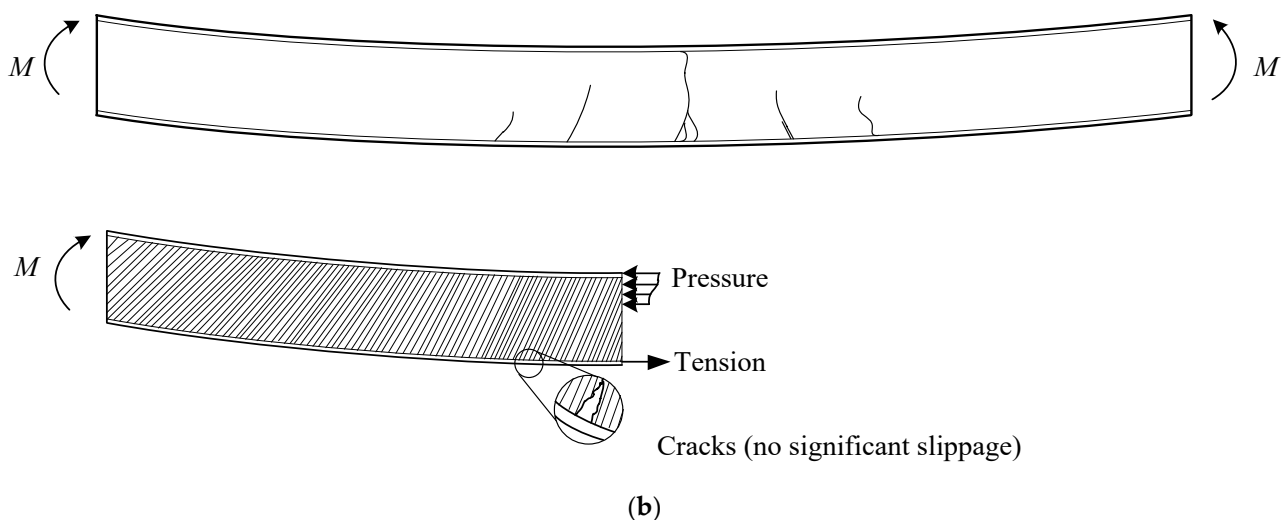
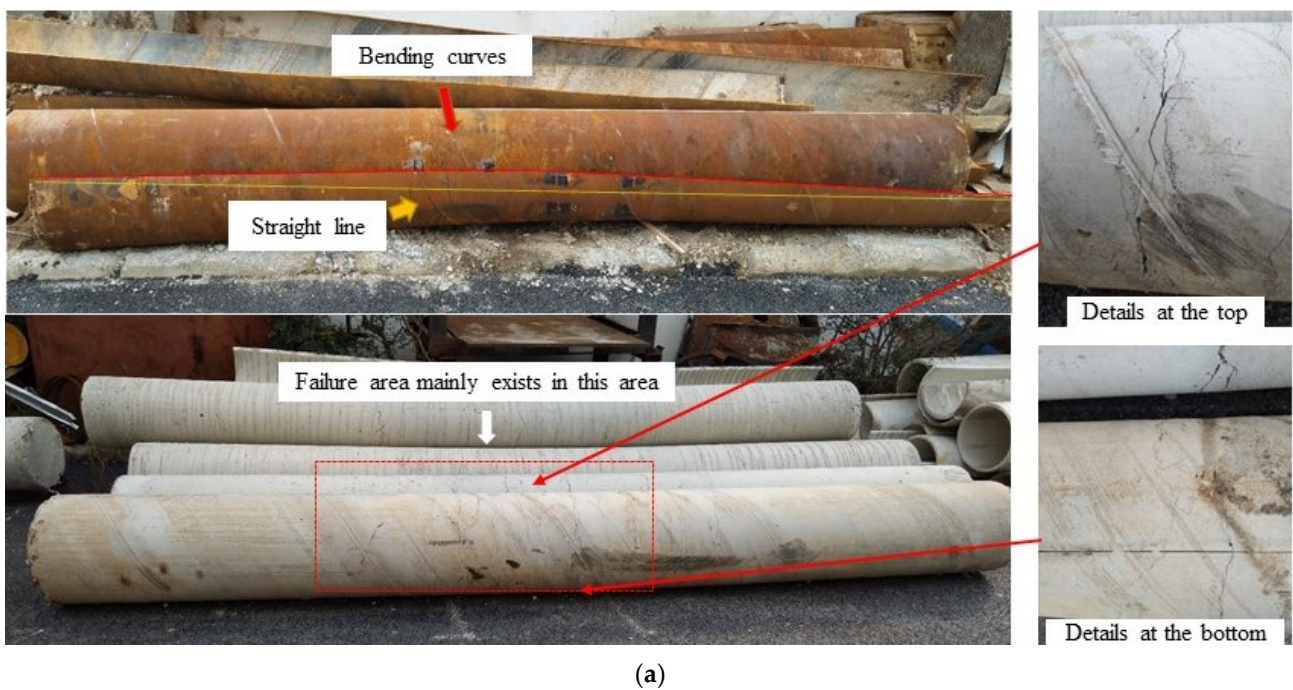


Figure 8. (a) Bending deformation and (b) cracks.

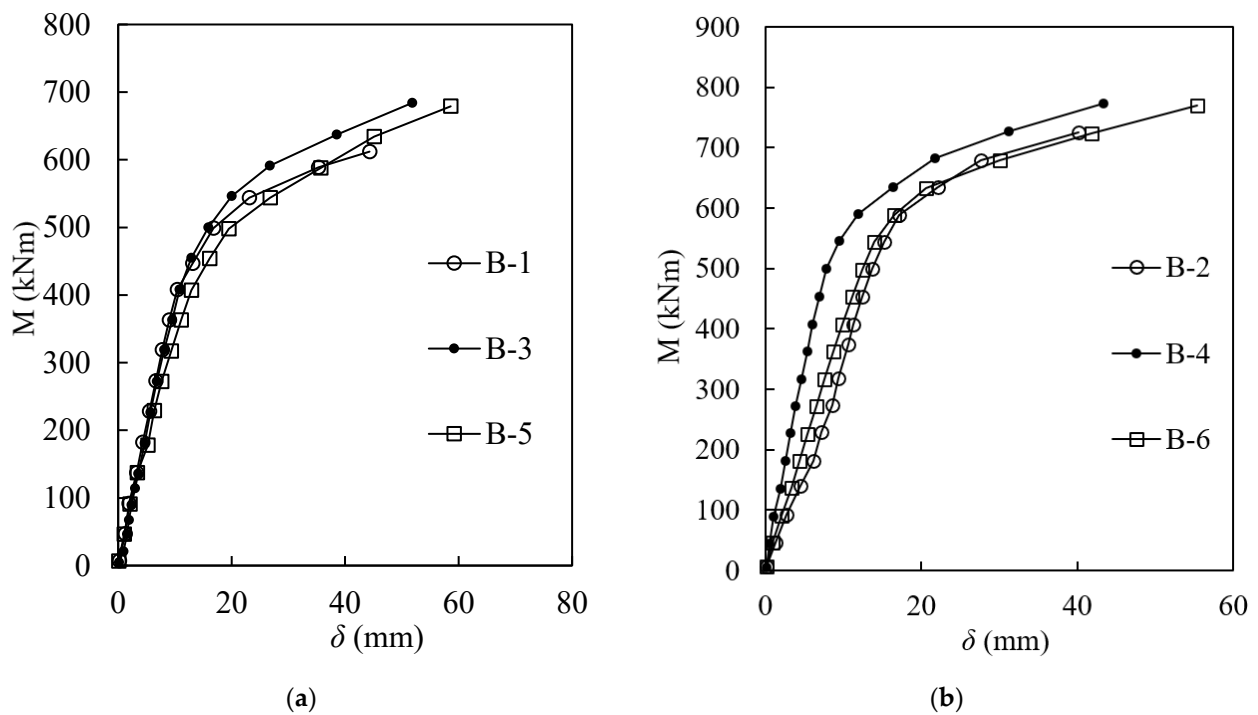


Figure 9. The bending moment-deflection curves of beams with different slurry conditions with (a) $t = 5$ mm and (b) $t = 10$ mm.

3.3.2. Effect of the Casing Thickness

The effect of the casing thickness on the moment capacity is shown in Figure 10. The thickness of the steel casing influenced the ultimate bending capacity and the elastic stiffness. The ultimate bending capacity of the composite beams increased from 549.1 kNm to 643.4 kNm, 588.9 kNm to 634.2 kNm, and 543.6 kNm to 679.5 kNm, as shown in Figure 11a–c, respectively, when the thickness of the steel casing increased from 5 to 10 mm. These increases in the ultimate bending capacities of the specimens were caused by the increase in the resistance when tensor failure occurred in the concrete parts of the beam. The increase in the steel casing thickness also enhanced the elastic stiffness and ductility. Therefore, the influence of casing thickness should be considered in the calculation of the section stiffness of the DSPC.

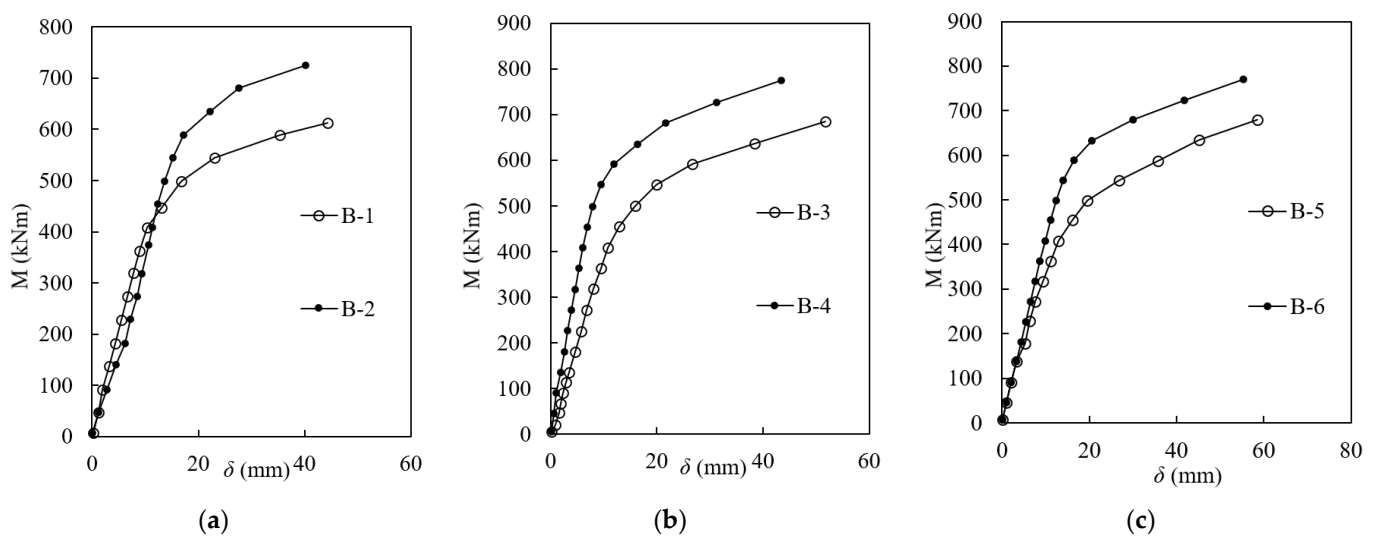


Figure 10. The effect of the casing thickness on the moment capacity of specimens: (a) no slurry, (b) thicker slurry, and (c) thickest slurry conditions.

3.4. Strain along the Pile Section

Strain gauges at the surface of the casing and in the concrete were used to measure the strain of the specimens. The changes in strain along the pile section of different specimens are shown in Figure 11. The strain along the height of the pile section of specimen B1 at different loading steps is presented in Figure 11a. The axis line of the pile was at the height of 213 mm. It is obvious that the strain above the neutral plane was negative, which indicates the pressure area of the specimens; furthermore, the strain below the neutral plane was positive, which presents the tensile area of the specimen section. The strain of the casing and concrete is linearly distributed at the initial loading stage, which means that the casing and the concrete body of the pile deformed as an assembly; thus, the plane cross-section assumption was reasonable at this stage. However, with increasing loading, the nonlinear layout became more obvious, which means that the plane cross-section assumption was no longer suitable. A similar conclusion can also be found in Figure 11b.

On the other hand, in Figure 11c–f, the strain of the casing and the concrete was in a nonlinear relationship at the beginning, which indicates that the plane cross-section assumption was no longer suitable. The difference in the y -axis between the casing and the concrete body was approximately 5–15%. This means that a significant difference in strain occurred between the steel and the concrete at the same loading stage. This, however, did not seem to lower the moment capacity of the specimens. This would have a significant negative effect on the bending stiffness of the member, especially for the plane cross-section assumption.

Compared with Figure 11, we can conclude that the existence of slurry had a negative effect on the bond properties between the steel casing and the concrete of the specimens, and in this case, the plane cross-section assumption was no longer suitable.

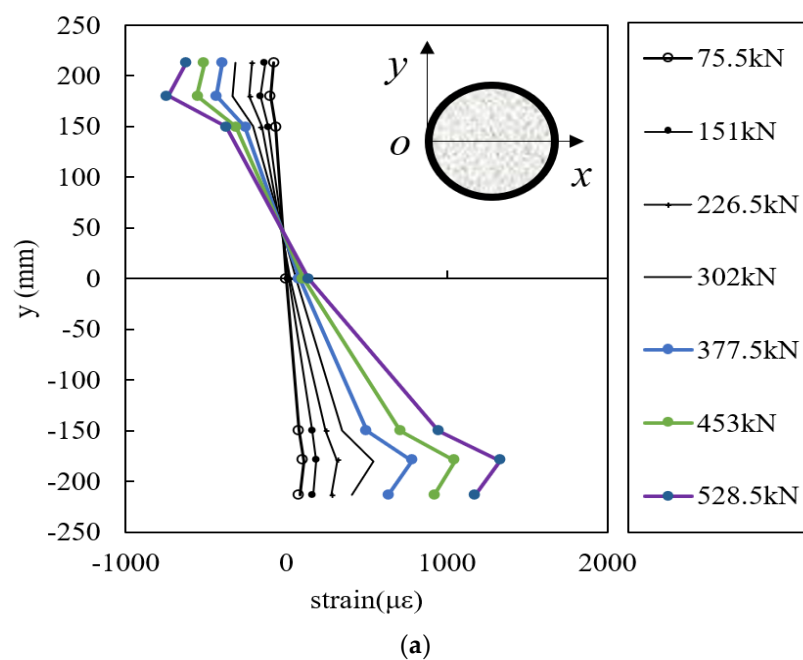


Figure 11. Cont.

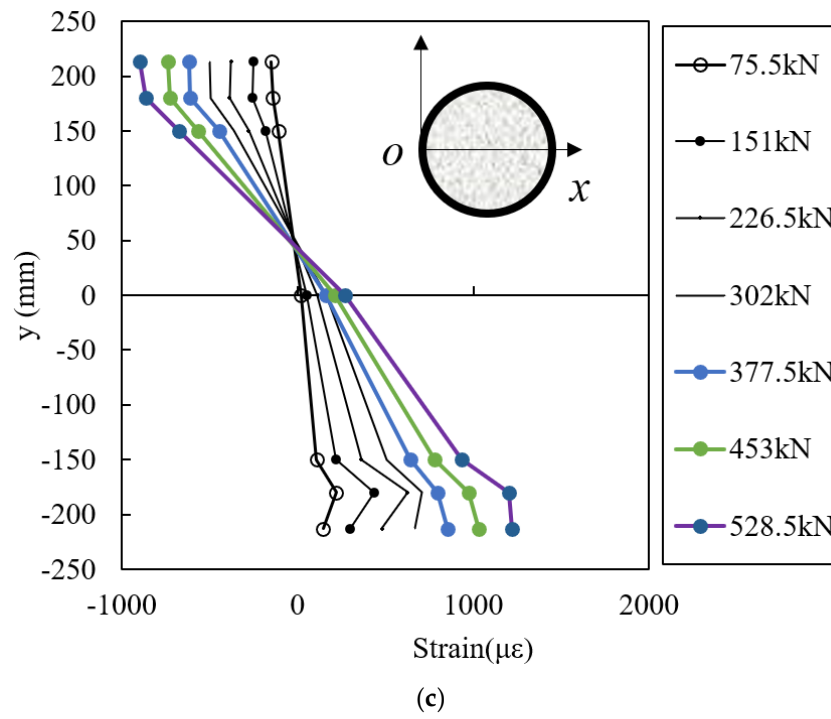
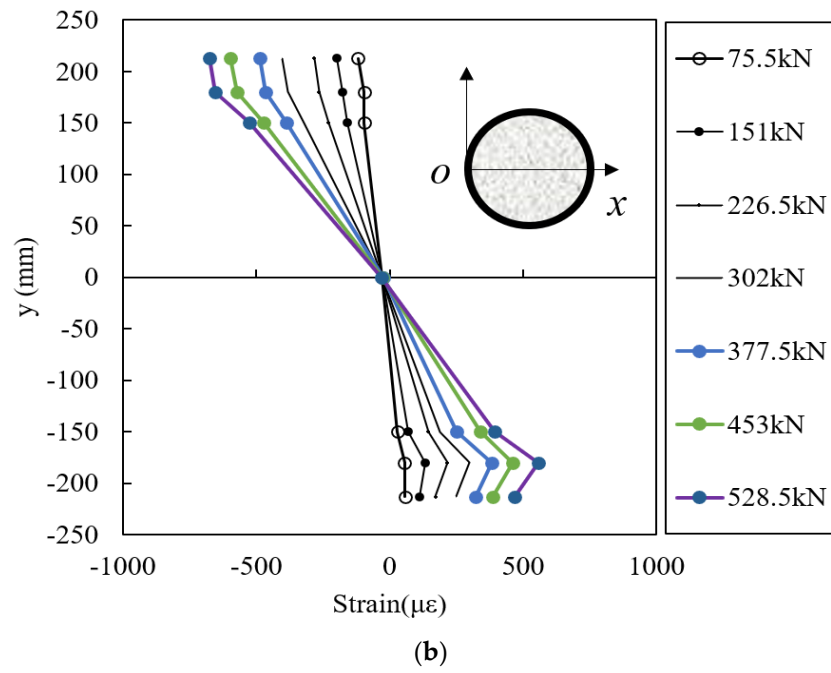


Figure 11. Cont.

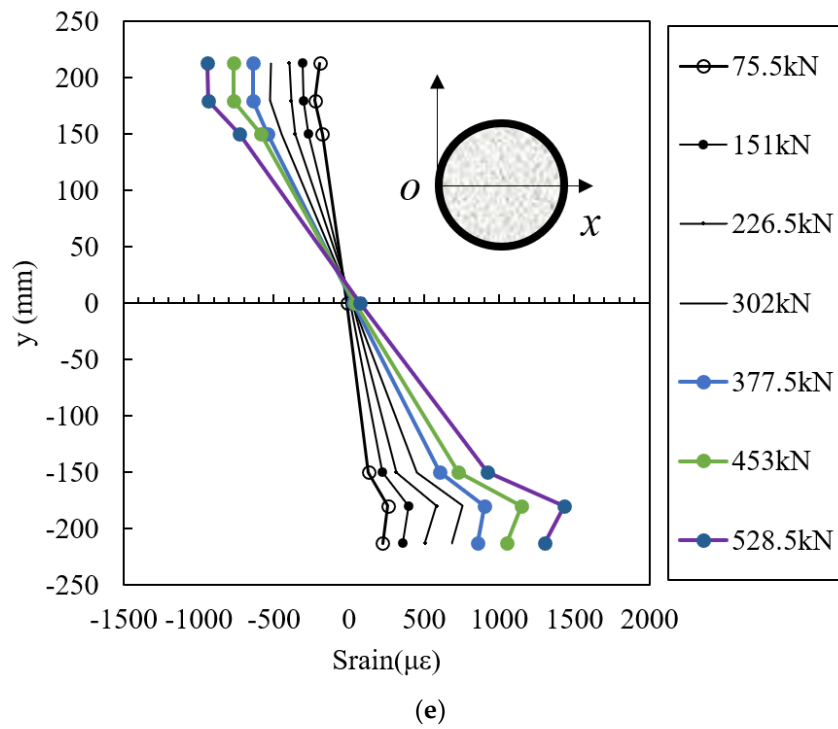
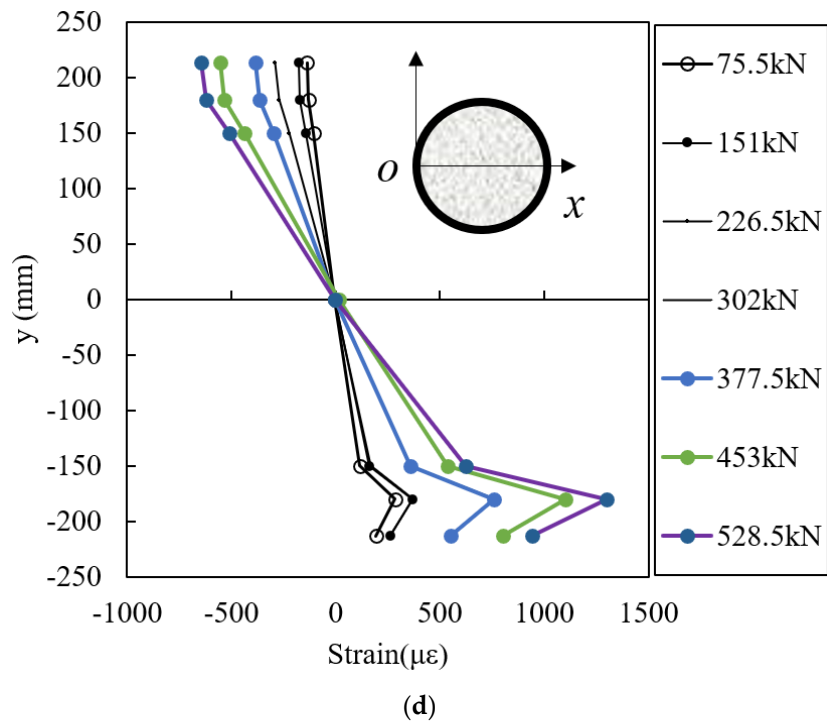


Figure 11. Cont.

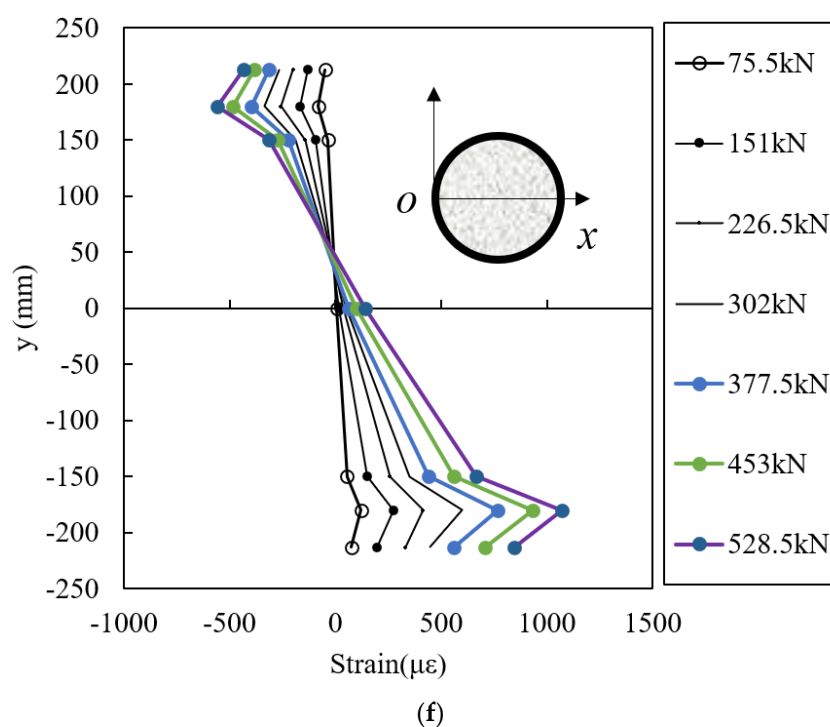


Figure 11. The changes of strain along pile section of different specimens: (a) B-1, (b) B-2, (c) B-3, (d) B-4, (e) B-5, and (f) B-6.

4. Conclusions

An in situ test and a series of laboratory experiments were implemented to investigate the bending behavior of DSPCs. On the basis of the experimental results, the following conclusions can be drawn:

- (1). In the field test, with the increase of the loads, there was no relative displacement between the concrete and the casing, and the casing and the concrete body of the pile deformed as an assembly. Therefore, it was suitable to use the plane cross-section assumption in the calculation. However, a correction coefficient that related to the loading level needed to be considered in the calculation of the bending stiffness.
- (2). From the laboratory studies, the bending capacities of those specimens were similar, the slurry condition had limited influence on the moment capacity of the specimens in terms of elastic stiffness and ductility, and the slurry condition had a negative influence on the bond quality. The plane cross-section assumption was reasonable to use in the calculation of bending capacity at low bending moments, and the influence of the casing thickness should be considered in the calculation of the section stiffness of DSPCs.

Author Contributions: Conceptualization, X.L. and G.D.; methodology, X.L.; validation, X.L.; formal analysis, X.L.; investigation, X.Y.; resources, G.D.; data curation, Q.Y.; writing—original draft preparation, X.L.; writing—review and editing, W.Z. and F.Z.; visualization, G.D.; supervision, G.D.; project administration, G.D.; funding acquisition, G.D. All authors have read and agreed to the published version of the manuscript.

Funding: This research was funded by the National Natural Science Foundation of China, project number 51878160, 52078128, the Natural Science Foundation of Jiangsu Province, project number BK20180155. The authors are grateful for their support.

Institutional Review Board Statement: Not applicable.

Informed Consent Statement: Not applicable.

Data Availability Statement: The data presented in this study are available on request from the corresponding author. The data are not publicly available due to the nature of this research.

Conflicts of Interest: The authors declare no conflict of interest. The funders had no role in the design of the study; in the collection, analyses, or interpretation of data; in the writing of the manuscript or in the decision to publish the results.

References

1. Lacki, P.; Derlatka, A.; Kasza, P. Comparison of steel-concrete composite column and steel column. *Compos. Struct.* **2018**, *202*, 82–88. [[CrossRef](#)]
2. Tao, Z.; Song, T.-Y.; Uy, B.; Han, L.-H. Bond behavior in concrete-filled steel tubes. *J. Constr. Steel Res.* **2016**, *120*, 81–93. [[CrossRef](#)]
3. Yuan, H.; Dang, J.; Aoki, T. Behavior of partially concrete-filled steel tube bridge piers under bi-directional seismic excitations. *J. Constr. Steel Res.* **2014**, *93*, 44–54. [[CrossRef](#)]
4. Chen, Y.; Feng, R.; Shao, Y.; Zhang, X. Bond-slip behaviour of concrete-filled stainless steel circular hollow section tubes. *J. Constr. Steel Res.* **2017**, *130*, 248–263. [[CrossRef](#)]
5. Lyu, W.-Q.; Han, L.-H. Investigation on bond strength between recycled aggregate concrete (RAC) and steel tube in RAC-filled steel tubes. *J. Constr. Steel Res.* **2019**, *155*, 438–459. [[CrossRef](#)]
6. Prion, H.G.L.; Boehme, J. Beam-column behaviour of steel tubes filled with high strength concrete. *Can. J. Civ. Eng.* **1994**, *21*, 207–218. [[CrossRef](#)]
7. Viridi, K.S.; Dowling, P.J. *Bond Strength in Concrete Filled Circular Steel Tube*; R. CESLIC Report CC11; Department of Civil Engineering, Imperial College: London, UK, 1975.
8. Wang, Z.-B.; Tao, Z.; Han, L.-H.; Uy, B.; Lam, D.; Kang, W.H. Strength, stiffness and ductility of concrete-filled steel columns under axial compression. *Eng. Struct.* **2017**, *135*, 209–221. [[CrossRef](#)]
9. Chen, W.F. Behaviour of concrete-filled steel tubular columns. In Proceedings of the International Conference on Tall Buildings, American Society of Civil Engineers and International Association for Bridge and Structural Engineering, Bethlehem, PA, USA, 21–26 August 1972; pp. 608–612.
10. Chen, W.F.; Atsuta, T. Theory of beam-columns. In *Volume I: In-Plane Behaviour and Design*; McGraw-Hill: New York, NY, USA, 1976; pp. 413–417.
11. Chen, W.; Chen, C. Analysis of concrete-filled steel tubular beam-columns. *Mem. Int. Assoc. Bridge Struct. Eng.* **1973**, *33*, 37–52. [[CrossRef](#)]
12. Nezamian, A.; Al-Mahaidi, R.; Grundy, P. Bond strength of concrete plugs embedded in tubular steel piles under cyclic loading. *Can. J. Civ. Eng.* **2006**, *33*, 111–125. [[CrossRef](#)]
13. GB 50936-2014. *Technical Code for Concrete Filled Steel Tubular Structures*; MOHURD: Beijing, China, 2014.
14. AIJ-2009. *Recommendations for Design and Construction of Concrete Filled Steel Tubular Structures*; Architectural Institute of Japan: Tokyo, Japan, 2009.
15. Eurocode 4 (EC4). Design of steel and concrete structures. In *Part 1 1: General Rules and Rules for Building*; European Committee for Standardization: Brussels, Belgium, 2004.